

Transient Vortex Events in the Initial Value Problem for Turbulence

D. D. Holm*

T-Division and CNLS, MS-B284, Los Alamos National Laboratory, Los Alamos, New Mexico 87545

Robert Kerr†

Department of Mathematics, University of Arizona, Tucson, Arizona 85721

(Received 18 October 2001; published 29 May 2002)

A vorticity surge event that could be a paradigm for a wide class of bursting events in turbulence is studied. The coherent mechanism is characterized by locally transverse vortex configurations that are intrinsically helical in both physical and Fourier space when there is a peak of the maximum vorticity $\|\omega\|_\infty(t)$. At no time are nonhelical, antiparallel vorticity elements observed. This event precedes the appearance of the traditional signatures of an energy cascade such as strong growth of the dissipation, spectra approaching $-5/3$, and strongly Beltramized vortex tubes. Comparing how different large-eddy simulations reproduce these properties demonstrates the importance of properly modeling nonlinear transport of both energy and helicity.

DOI: 10.1103/PhysRevLett.88.244501

PACS numbers: 47.27.Cn, 47.27.Eq

Although three-dimensional turbulence is characterized by intermittent events both in space and time, it is often envisaged as a homogeneous, statistically steady tangle of vortex tubes accompanied by a steady transfer of energy through the spectrum to high wave numbers and a $k^{-5/3}$ energy spectrum. This statistically steady description has been used to verify turbulence models through simulations of forced turbulence and decaying homogeneous, isotropic turbulence [1,2]. In these studies, it is sometimes argued that the initial nonequilibrium transients can be ignored as being nonuniversal. However, each intermittent burst of turbulence is itself a transient dynamical process involving individual vortex interactions whose ensemble average is responsible for the overall statistical properties. Our objective is to apply a coordinated set of diagnostics in both physical and wave number space for numerically detecting individual vortex surge events and their effects upon the subsequent dynamics.

The numerical investigation of the decay of turbulence discussed here is designed to improve our understanding of individual intermittent events and continues a long tradition in numerical modeling of the initial value problems in computational fluid dynamics. Numerically, the question of transient phenomena in turbulence has been considered previously using a variety of initial conditions [3–7]. In this Letter the evolution from smooth, random, initial conditions introduced in [5] to steady turbulent decay is considered using this coordinated set of diagnostics. These diagnostics show that this initial value problem for turbulence evolves through several complex states in a sequence of transitions. These include the following: (i) Formation of vortex sheets that interact, encounter each other transversely, and then begin to roll up into vortex tubes. (ii) Development of a peak in the maximum vorticity $\|\omega\|_\infty(t)$ that is correlated with helicity signatures in both physical and wave number space. (iii) Rearrangement of vortex tubes into transverse pairs

having oppositely signed helicity $\Lambda = \mathbf{u} \cdot \boldsymbol{\omega}$, where vorticity $\boldsymbol{\omega} = \text{curl} \mathbf{u}$. Unlike inviscid configurations [7], the velocity \mathbf{u} on each tube of the pair is only partially induced by its partner. Instead, \mathbf{u} on the tubes arises primarily as a response to strains and dissipation distributed within the pair. (iv) formation of the classical decay regime with a $k^{-5/3}$ energy spectrum.

While our analysis also includes traditional diagnostics such as energy decay, our new understanding will arise primarily through the time evolution of the maximum vorticity in Fig. 1, physical space visualizations in Figs. 2 and 5, helicity probability distributions in Fig. 3, and the accompanying helicity cospectrum in Fig. 4. Central to our new understanding is the following observation: although this initial condition is not a Beltrami flow, spatial regions develop early during its evolution where the helical alignment measured by $\cos\theta = \Lambda/(u\omega)$ of either sign is locally near unity in magnitude. Evidence is given that the ensuing dynamics is influenced by helicity Λ , whose evolution depends upon the interplay between nonlinear transport terms, viscous effects and large-eddy stress parametrizations.

The time scale for this investigation is set by a surge in the growth of the maximum vorticity at $t = 0.5$ in Fig. 1. This time scale also appears in three 64^3 results: the 256^3 direct numerical simulation (DNS) filtered onto a 64^3 mesh, in a Smagorinsky calculation using a traditional eddy viscosity model, and in a calculation using the new Lagrangian-averaged Navier-Stokes (LANS)- α model, which preserves nonlinear transport properties (see [8] and references therein). The growth of vorticity comes from the vortex stretching terms, which at early times involves only large-scale strain and, thus, should not be affected by the small scales. Evidence that vortex stretching at early times is not strongly affected by the small scales is that all three calculations have the same time scale $t = 0.5$ for the vorticity surge. The differences among

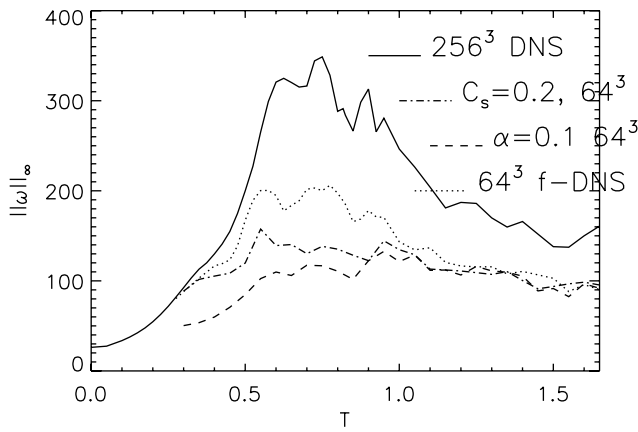


FIG. 1. Comparison of the growth of $\|\omega\|_\infty$ between our 256^3 direct numerical simulation and three results on 64^3 meshes. The full 256^3 DNS filtered onto a 64^3 mesh, labeled 64^3 f-DNS, a 64^3 traditional Smagorinsky eddy viscosity model, and a calculation using the LANS- α model. This figure sets the time scales for our analysis.

the calculations should therefore be due to how vorticity is suppressed by either viscous effects or large-eddy simulation (LES) model effects. The identical growth in $\|\omega\|_\infty$ in each case until $t = 0.3$ tells us that until that time dissipation and LES parametrization have not yet affected the calculations.

It has previously been shown that the dominant initial structures are vortex sheets that arise out of non-Beltrami initial conditions [5]. From the interaction of those initial vortex sheets in the weakly dissipative regime, Fig. 2

$\omega > .55\omega_p$, ω lines, $t=0.5$
blue: $H < -300$, green: $H > 300$

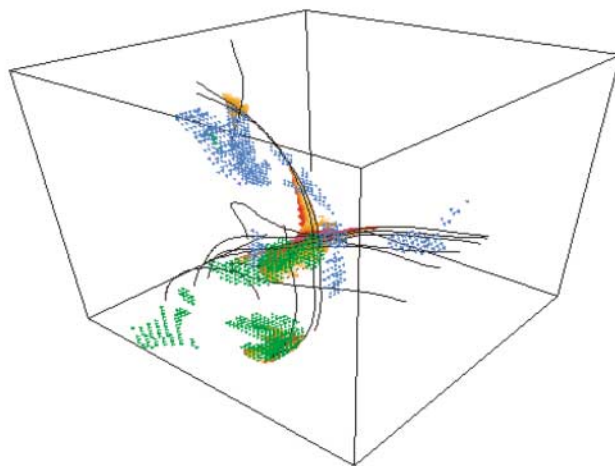


FIG. 2 (color). Isosurfaces of vorticity at $t = 0.5$ where $\omega \geq 0.55\|\omega\|_\infty$ in red/earth colors with sample vortex lines through these regions. Regions of high positive and negative helicity are indicated by green and blue, respectively. The vortex lines meet transversely, which is an inherently helical configuration.

shows that a new configuration of transversely aligned vortex structures has formed by $t = 0.5$. We will demonstrate that this is an inherently helical configuration that has arisen from the non-Beltrami initial conditions simultaneously with the vorticity surge event. The helical nature of the configuration is shown both by the concentrations of helicity density Λ near the vortex structures in Fig. 2 and by a skewed, transient probability density distribution (PDF) of the cosine of the helicity angle at $t = 0.5$ in Fig. 3. Accompanying this helicity signature in physical space, the helicity cospectrum at low wave numbers in Fig. 4 develops a strong signature of alternating sign between wave number bands. This is evidence for the dynamical formation of large, asymmetrical distributions of helicity associated with the vorticity surge in Fig. 1.

While the helicity density is not Galilean invariant, Galilean transformations cannot remove the strong fluctuations in helicity in physical space that we observe, nor could they remove the strong fluctuations in the helicity cospectrum in Fig. 4. The implication is that if these are configurations that naturally and frequently arise in a turbulent flow, then helicity could be playing a central role in their dynamical evolution. The PDF of the helicity angle in Fig. 3 quickly changes into a distribution with peaks concentrated at $\cos\theta = \pm 1$ as reported in other turbulent flows [9,10]. The appearance of the individual peaks is associated with the formation of nearly Beltrami vortex tubes by $t = 0.7$, shown in Fig. 5.

The association of the vorticity surge with helicity raises some important questions about the absence of antiparallel

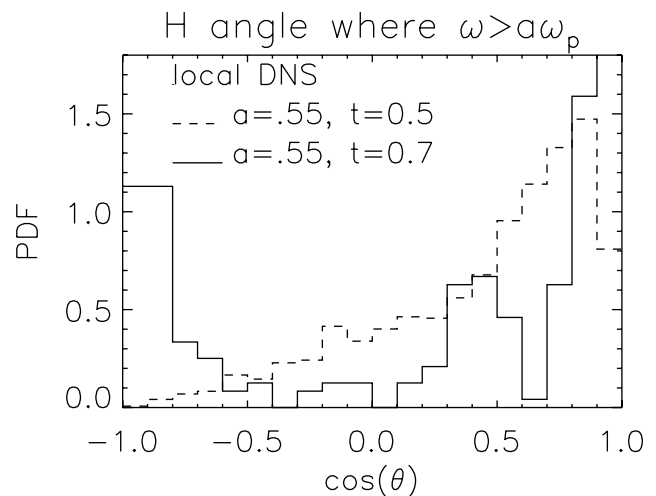


FIG. 3. Probability density functions of the helicity angle $\cos\theta = \hat{u} \cdot \hat{\omega} / u\omega$ in physical space at $t = 0.5$, during the surge in the vorticity maximum, and $t = 0.7$ after formation of the first distinct vortex tubes. The distribution is taken over those points with vorticity above the shown threshold, 55% of the maximum vorticity $\omega_p = \|\omega\|_\infty$, in the subdomain containing $\|\omega\|_\infty$ at both $t = 0.5$ and $t = 0.7$. The distribution was initially flat. The asymmetry in the distribution emerges because the transverse vortex configurations that develop are inherently helical.

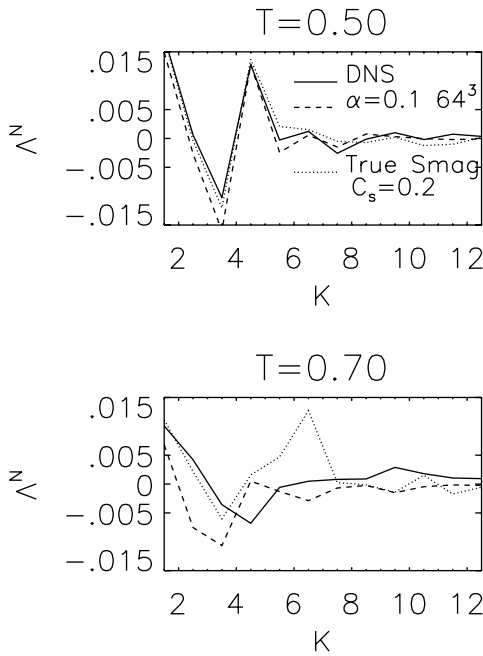


FIG. 4. Comparison of the normalized helicity cospectra $\Lambda^N(k)$ for two times. The normalization is based upon the energy and enstrophy at each time so that comparisons in magnitudes between the different calculations can be made. These strong oscillations first appear at $t \approx 0.45$ when dissipation is still negligible and the vortex structures are beginning to change from sheets to tubes via a roll-up instability induced by interactions between distinct vortex sheets. The higher wave number oscillations disappear as soon as dissipation becomes significant.

vorticity elements. In the inviscid limit, antiparallel vorticity elements around the position of the maximum vorticity $\|\omega\|_\infty$ were thought to lead to the strongest increases in vorticity [6,11]. In a strictly antiparallel configuration there would be equal concentrations of both signs of the helicity, which would cancel at each length scale and thus preclude any spectral oscillations.

Instead, at no time during this calculation are the most intense vorticity elements observed to be antiparallel. The calculations that suggest that the antiparallel configuration would be dominant are all based upon inviscid calculations using vortex filaments and tubes (see [11] and references in [7]). The spectral calculations reported here, which are viscous and initially develop vortex sheets, show no such trend.

Isolated, helical vortex tubes first form immediately after the vorticity surge at $t = 0.5$. The helical character of these vortex tubes is demonstrated by physical space renderings that show that the strongest helicity fluctuations are clearly tied to vortex tubes in Fig. 5 at $t = 0.7$ and by strong peaks at both 1 and -1 in the helicity distribution in Fig. 3. This PDF was centered upon the domain shown. Note that the two dominant tubes have opposite signs of helicity. Rotating one's view of this local region shows that the tubes are nearly orthogonal and when the entire

$\omega > .47\omega_p$, ω lines, blue:H<0, green:H>0, DNS $t=0.7$

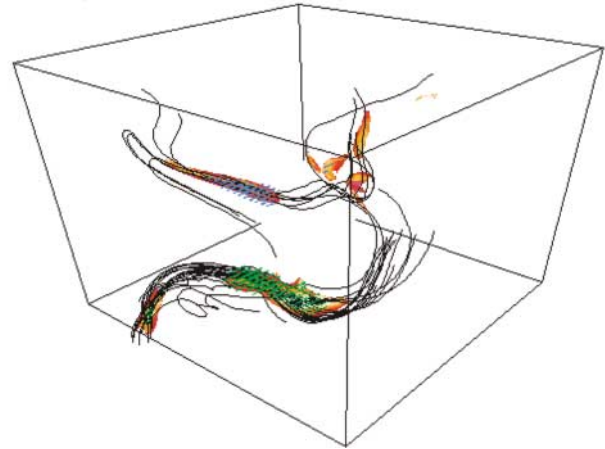


FIG. 5 (color). Isosurfaces of vorticity at $t = 0.7$ where $\omega \ge 0.47\|\omega\|_\infty$ in red/earth colors with sample vortex lines through these regions. Regions of high positive and negative helicity are indicated by green and blue, respectively. The visualization volume is centered on the new maximum vorticity and rotated with respect to Fig. 2 to emphasize the Beltrami nature of the vortex tubes. From another angle, it can be seen that the transverse alignment found in Fig. 2 persists.

flow is rendered, this configuration appears in a localized corner $1/4^3$ of the entire domain. This demonstrates that these structures are interacting strongly within this localized region. As time goes on, vortex tubes whose helicity is opposite develop as orthogonal pairs in many localized regions. This is not the first time that nearly orthogonal configurations of vortex tubes have been created in direct simulations. They have appeared in renderings going back to about the mid-1980s [3,12]. The new point we are making is that this intrinsically helical configuration arises in conjunction with the vorticity surge.

The rapid development of structures characteristic of fully developed turbulence by $t = 0.7$ from the helical state at $t = 0.5$ occurs simultaneously with the disappearance of the intermediate peak in the helicity cospectrum in Fig. 4 seen at $t = 0.5$. The wave number ($k = 5$) of this peak at $t = 0.5$ is too low for the disappearance to be a direct effect of viscosity. Instead, we believe it is due to a combined effect of transfer to larger wave numbers, followed by dissipation at those larger wave numbers. The evidence for this is the different manner in which the two large-eddy simulations treat the nonlinear transfer of helicity. The LANS- α model preserves the transport of helicity. Consequently, when energy is transported to small scales and is dissipated, so should any helicity that accompanies that energy. This is consistent with the observation in Fig. 4 that the intermediate peak in its helicity cospectrum disappears by $t = 0.7$. Graphics also show vortex structures consistent with the large-scale structures in the DNS.

For Smagorinsky, the intermediate peak in the helicity cospectrum that had formed by $t = 0.5$ persists, only

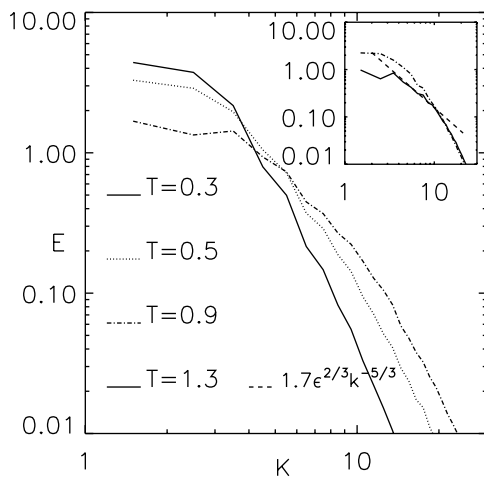


FIG. 6. Comparison of the energy spectra versus the three-dimensional wave number by shells for several times. The main figure shows spectra up to $t = 0.9$. Between $t = 0.3$ and $t = 0.5$, the high wave numbers are filled and there is little decrease in the overall energy. Between $t = 0.5$ and $t = 0.9$, there is a significant decrease in the energy in the lowest wave numbers. The expected $k^{-5/3}$ law establishes itself by $t = 1.3$, as shown by the inset.

moving slightly towards higher wave numbers by $t = 0.7$. There are no assurances in the Smagorinsky model that both helicity and energy will be dissipated. In fact, Smagorinsky can generate anomalous helicity. Furthermore, clearly defined vortex tubes have not formed at this time in the Smagorinsky calculation. Hence, the proper spectral dynamics of helicity and the formation of vortex tubes are part of one nonlinear process involving diffusion, stretching, and proper transport. This implies that a large-eddy simulation that has correct transport properties is required to capture this process.

Once the interacting, transversely aligned, helical vortex tubes have formed, dissipation grows rapidly in the DNS and as has been reported [5] and shown in Fig. 6, the kinetic energy spectrum $E(k)$ gradually approaches the classical $k^{-5/3}$ characteristic of a turbulent energy cascade. Once a clear $-5/3$ spectrum appears near $t = 1.3$, the energy decay becomes self-similar [4].

Interactions between regions or modes of oppositely signed helicity have previously been investigated in the context of shell models. In one of the most popular shell models, the Gledzer-Ohkitani-Yamada (GOY) model, the sign of helicity in each shell alternates. It has been shown that the GOY interactions are consistent with one channel in a helical decomposition of the energy transfer [13,14]. This analysis also shows that the strongest wave number interactions occur between modes of opposite helicity. In DNS calculations it has been shown that helicity can arise from nonhelical initial conditions and that energy and he-

licity can move together to high wave numbers and be dissipated [14,15].

We conclude that dynamics involving helicity dynamics is essential during an early stage in establishing the turbulent energy cascade from smooth initial conditions. The new features that we emphasize are the formation of a helical state in association with the vorticity surge and how this state rapidly develops into the structures and distributions that set the stage for fully developed turbulence. We believe that understanding this transition could be important in the parametrization of transient events in turbulence. Such transitions must influence the overall statistical properties controlled by intermittent, intense events. Evidence was presented that the mechanism by which classical vortex tubes first form requires both transport and dissipation and that this implies that large-eddy parametrizations should preserve some of these helicity transport properties. In ongoing work we are investigating the capabilities of several modern approaches to large-eddy simulation in representing these helicity transport properties.

We are grateful to many friends for their enormous help in supplying suggestions, advice, and encouragement during the course of this work. In particular, several helpful and timely discussions with S. Y. Chen, G. Eyink, U. Frisch, and K. Sreenivasan especially influenced this work.

*Email address: dholm@lanl.gov

†Email address: kerr@math.arizona.edu

- [1] R. A. Clark, J. H. Ferziger, and W. C. Reynolds, *J. Fluid Mech.* **91**, 1 (1979).
- [2] S. Y. Chen, D. D. Holm, G. Margolin, and R. Zhang, *Physica (Amsterdam)* **133D**, 66 (1999).
- [3] M. E. Brachet, D. I. Meiron, S. A. Orszag, B. G. Nickel, R. H. Morf, and U. Frisch, *J. Fluid Mech.* **130**, 411 (1983).
- [4] S. Kida and Y. Murakami, *Phys. Fluids* **30**, 2030 (1987).
- [5] J. R. Herring and R. M. Kerr, *Phys. Fluids A* **5**, 2792 (1993).
- [6] R. M. Kerr, *Phys. Fluids A* **5**, 1725 (1993).
- [7] S. Kida and M. Takaoka, *Annu. Rev. Fluid Dyn.* **26**, 169 (1994).
- [8] C. Foias, D. D. Holm, and E. Titi, *Physica (Amsterdam)* **152D**, 505 (2001).
- [9] R. B. Pelz, V. Yakhot, S. A. Orszag, L. Shtilman, and E. Levich, *Phys. Rev. Lett.* **54**, 2505 (1985).
- [10] W. Polifke and L. Shtilman, *Phys. Fluids A* **1**, 2025 (1989).
- [11] A. Pumir and E. D. Siggia, *Phys. Fluids* **30**, 1606 (1987).
- [12] R. M. Kerr, *J. Fluid Mech.* **153**, 31 (1985).
- [13] F. Waleffe, *Phys. Fluids A* **5**, 677 (1993).
- [14] L. Biferale and R. M. Kerr, *Phys. Rev. E* **52**, 6113 (1995).
- [15] C.-N. Chen, S. Y. Chen, G. Eyink, and D. D. Holm, "Statistics of Helicity Flux in Fully Developed Turbulence" (to be published).